Chapter 9
Synthesis of Hydroxyapatite by Wet Method: Effect of Acid Solution Concentration on Powder Granulometry

Ouardia Zamoume and Rym Mammeri

Abstract Hydroxyapatite was obtained after heat treatment (600 °C) of the powder synthetized by neutralizing a solution of calcium hydroxide $Ca(OH)_2$ with phosphoric acid H_3PO_4 under atmospheric conditions and reduced time aging. The Ca/P molar ratio of the reagents was 2.0. The concentration of the solution of phosphoric acid influences the pH of the mixture and particle size distribution of solid products. When the $Ca(OH)_2$ solution was neutralized with concentrated phosphoric acid, the average particle size obtained is about 9.13 μm, whereas when the $Ca(OH)_2$ solution was neutralized with diluted solution of phosphoric acid, the average particle size is about 79.40 μm. Agglomerated particles were formed when phosphoric acid solution was used in diluted form. FTIR and DRX analyses have shown that the as-dried powder (at 100 °C) was a calcium carbonate–phosphate with low crystallinity, which after sintering at temperature higher than 600 °C leads to the formation of crystalline hydroxyapatite (HA) with CaO second phase in minor quantities. No decomposition of hydroxyapatite single phase was observed even at high temperature treatment of the powder (1100 °C).

Keywords Hydroxyapatite · Neutralization · Rich calcium solution · Thermal stability

1 Introduction

Hydroxyapatite $Ca_{10}(PO_4)_6(OH)_2$ (Ca/P = 1.67) is the most calcium phosphate used in biomedical field as biomaterial, adsorbent and catalytic support. As biomaterial, hydroxyapatite (HA) is bioactive, biocompatible, and osteoconductive but possesses a very low solubility in vivo. To overcome this problem, hydoxyapatite is sometimes associated with tricalcium phosphate (βTCP), which has good solubility. This biphasic material (HA/βTCP) combines the properties of HA and βTCP, and thus,

O. Zamoume (✉) · R. Mammeri
Faculty of Sciences, Department of Chemistry, University M'hammed Bouguara Boumerdes, Boumerdes, Algeria
e-mail: zamouar@yahoo.fr

D. Trache et al. (eds.), *Materials Research and Applications*,
Materials Horizons: From Nature to Nanomaterials,
https://doi.org/10.1007/978-981-15-9223-2_9

its resorption properties in vivo are improved. Hydroxyapatite biomaterial can be obtained by heat treatment of bones, which are composed by carbonated hydroxyapatite or by synthetic routes. Due to its low solubility, hydroxyapatite has a great stability in water, which is an important parameter for adsorbent materials. Hydroxyapatite crystallizes in hexagonal system ($P_{6/3\ m}$ space group), with a lattice parameters: $a = 9.37$ A° and $c = 6.86$ A°. Its structure is composed of PO_4^{3-}, Ca^{2+}, and OH^- ions, which can be substituted by monovalent, divalent, and trivalent ions. This ionic substitution capacity makes these materials very efficient in the field of wastewater treatment, removal of dyes, and chromatography (Maya et al. 2020). Hydroxyapatite possesses very good retention capacities for heavy metal ions such as Pb^{2+}, Cd^{2+}, Cr^{3+}…. (Haifeng et al. 2019; Michele et al. 2019). The retention capacities of heavy metals on surface of hydroxyapatite depend on the surface affinity of this material. Thus, the phosphate and hydroxyl groups in hydroxyapatite surface are hard Lewis bases and have good affinity for hard Lewis acid as lead cations. The ionic radii of the cation are another parameter on which depends the retention capacity. Cations with ionic radii bigger than Ca^{2+} are more likely to be incorporated in HA structure. In addition, hydroxyapatite with low crystallinity that corresponds to high surface area is more beneficial to remove heavy metal ions (Doan et al. 2012a, b; Sangeetha et al. 2018; Maya et al. 2020).

Hydroxyapatite can be prepared by many synthetic routes, which include dry methods, high-temperature processes, wet methods, etc. (Mehdi et al. 2013). Among these techniques, the most widely used one is the wet chemical route. The advantages of this method are that different particle sizes and morphologies can be obtained by varying the preparation conditions (Peipei et al. 2010; Elhammari et al. 2007). The common reagents used to synthesize hydroxyapatite are calcium nitrate and calcium chloride as calcium sources and ammonium orthophosphate salts as orthophosphate sources because of their high solubility in aqueous solutions. However, these reagents result in non-used ions as NO_3^-, Cl^-, K^+, and Na^+, which require several washing in order to eliminate them. Calcium hydroxyde and orthophosphoric acid seem to be good reagents for the synthesis of hydroxyapatite by an acid–base neutralization (Florin et al. 2017). This process results in any non-used ion and the reagents are available at low cost (Doan et al. 2014). Hydroxyapatite used as adsorbent is stoichiometric (Ca/P = 1.67). According to previous work, in order to obtain a stoichiometric hydroxyapatite, the molar ratio of the reagents must be equal to 1.67, the temperature of the reaction must be high (90 °C), and the aging time of the obtained precipitate must be long (above 24 h).

The objective of this work is to synthesize hydroxyapatite powder by acid–base neutralization at low temperature, reduced aging time, and different acid solution concentration. In these conditions and in order to obtain stoichiometric hydroxyapatite with a Ca/P = 1.67, the reagents were mixed in a molar ratio of 2 (Ca/P = 2). Based on the results of the analyses, the effect of phosphoric acid solution concentration on the pH of the suspension, the particle size distribution, and thermal stability of the Ca-HA are studied.

2 Materials and Methods

2.1 Reagents

The reagents were $Ca(OH)_2$ and H_3PO_4 (85%) in water. All of them were of high purity (99%) and purchased from Prolabo.

2.2 Synthesis Methods

2.2.1 Powder n°1 (P1)

A solution of $Ca(OH)_2$ was obtained by dissolution of 0.1 mol of $Ca(OH)_2$ in 500 mL of distilled water. The solution was stirred with a magnetic stirrer at 400 rpm and maintained at room temperature (23 °C). A volume of 3.2 mL of H_3PO_4 (85% wt., in water), at room temperature, was then added drop wise (1 mL/min) into the $Ca(OH)_2$ solution with a graduated burette. After the total addition of H_3PO_4, the mixture was continuously agitated for an additional one hour at the same temperature. The pH of the acid–base solution was monitored with pH meter. The precipitate was separated, washed several time with distilled water, filtered then dried à 100 °C during 24 h.

2.2.2 Powder n°2 (P2)

A solution of $Ca(OH)_2$ was obtained by dissolution of 0.1 mol of $Ca(OH)_2$ in 250 mL of distilled water. The solution was stirred with a magnetic stirrer at 400 rpm and maintained at room temperature (23 °C). 3.2 mL of H_3PO_4 solution was introduced in 250 mL of distilled water and then added drop wise (12.5 ml/min) into the $Ca(OH)_2$solution. The total time addition of H_3PO_4 solution was 20 min. The obtained precipitate was continuously agitated for an additional one hour at the same temperature. The obtained suspension was washed several times with distilled water, filtered then dried à 100 °C during 24 h.

In order to study their thermal stability, the as-dried powders are sintered at 600, 800, 1000, and 1100 °C in a furnace under air atmosphere, with a heating rate of 5 °C/min, kept for 1 h, and then the sample was cooled down to room temperature.

2.3 Characterization Methods

2.3.1 Powder X-ray Diffraction (XRD)

The phase composition of the as-synthesized and calcined powders was analyzed by X-ray diffraction with Philips XPERT PRO diffractometer using CuKα radiation (λ = 1.54056 Å) at the X-ray tube voltage 45 kV and a current of 40 mA. The X-ray data were collected over the 2θ range of 20–70° at a step size of 0.0167°.The average crystallite size of the precipitates was estimated from the Debye–Scherrer equation:

$$D_{\mathrm{hkl}} = \frac{K\,\lambda}{ß\cos\theta}$$

where D_{hkl} is the size (in nm), ß is the full width at half maximum of the peak at half of the maximum intensity, FWHM (in degree), λ is the diffraction wavelength of X-rays (1.5418 Å), θ is the diffraction angle for each reflection, and K the shape factor equals to 0.94.

2.3.2 Particles Size Distribution

A particle size analyzer (Malvern Mastersizer 2000) was used to determine the size distribution of the powder samples.

2.3.3 FTIR Spectroscopy

The typical groups of the synthesized and calcined powders were identified by Fourier-transform infrared spectroscopy (FTIR-4100//ATR ESPECAC). The measurements were obtained at 400–4000 cm^{-1} with a resolution of 0.4 cm^{-1}.

2.3.4 Elementary Analysis

The elemental analysis was performed by fluorescence X spectroscopy (Magix PRO, PW 2540 vrc).

3 Results and Discussions

As shown in Fig. 1, the pH of the mixture varies slowly with time when the phosphoric acid solution used is in concentrated form (pH ≈ 12.3), whereas when the phosphoric acid solution used for neutralization is diluted, the pH of the mixture was slowed

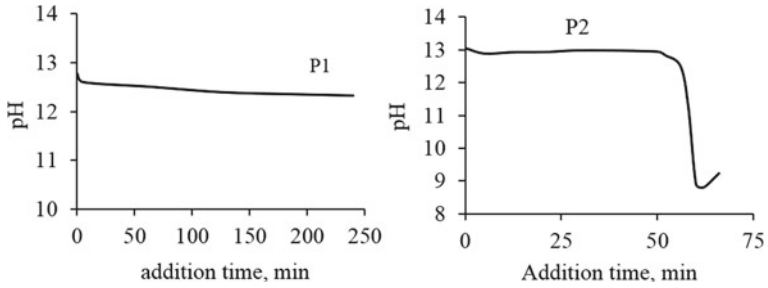

Fig. 1 Evolution of pH with time addition of phosphoric acid to $Ca(OH)_2$ solution

down to 8.8. These results indicate that the formation mechanism of the powders P1 and P2 is different. Indeed, at a pH of 12.3, the predominant species in solution are PO_4^{3-} ions, while at a pH of 8.8, there are both PO_4^{3-} and HPO_4^{2-}.According to the results showed in Table. 1, the Ca/P molar ratio of powder P2 (Ca/P = 1.20) is higher when compared to powder P1 (Ca/P = 1.15), which can be due to a more substitution of PO_4^{3-} groups by CO_3^{2-}.

The X-ray diffraction patterns of the as-dried powders are similar as shown in Fig. 2. All the peaks are identified and correspond to HA phase (ICDD N°96-900-2217). The broad and weak peaks diffraction indicates that the powder is a poorly crystallized apatitic phosphate with small crystallite size. This is confirmed by the

Table 1 Ca/P molar ration of as-dried powders P1 and P2 at 100 °C and 24 h

Powder	Ca (wt %)	P (wt%)	Ca/P	Ca/P (molar ration)
P1	48.93	32.88	1.48	1.15
P2	52.74	33.81	1.55	1.20

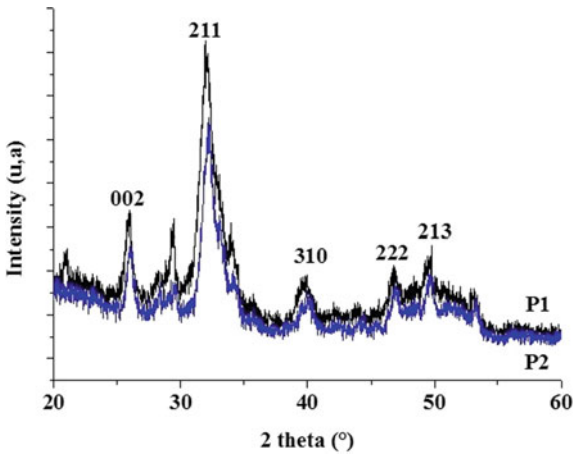

Fig. 2 XRD patterns of as-dried powder P1 and P2 at 100 °C for 24 h

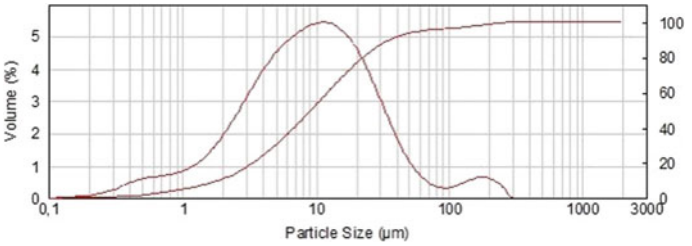

Fig. 3 Particle size distribution of as-dried powder P1 at 100 °C and 24 h

crystallite sizes estimated from the Debye–Scherrer equation, which are about 8.77 and 10.20 nm for powder P1 and P2, respectively. The low crystallinity of the formed apatitic phosphate can be attributed to the low synthesis temperature used (Elhammari et al. 2007; Elena et al. 2004), which lead to fast precipitation that prevented the crystallization. Moreover, the presence of B-carbonate in anapatite lattice causes a decrease in crystallinity (Elena 2004). Souzaa et al. (2019) showed that the amorphous calcium phosphate (ACP) is very reactive, thus adsorbs atmospheric CO_2 and forms a carbonated apatite.

The particle size distribution of the powder P1 is homogeneous (Fig. 3). 90% of particles have smaller size than 34.85 µm (d_{90}), and 50% of them present smaller size than 9.13 µm (d_{50}). Visually and during synthesis process, the precipitate P2 formed has spherical agglomerates compared to the precipitate P1, which has a very fine appearance. The formation of agglomerates in the case of powder P2 was confirmed by particle size analyses (Fig. 4), which showed that 90% of particles have smaller size than 350.23 µm (d_{90}), and 50% (d_{50}) of them present smaller than 79.40 µm. Our results are not really in agreement with those obtained by Azade and Suat (2018), who have shown that slow or rapid addition of H_3PO_4 to $Ca(OH)_2$ solution has no influence on the particles size distribution.

The FTIR spectra of the as-dried powders P1 and P2 are shown in Fig. 5. All the bands detected for powder P1 are characteristics of functional groups of an apatitic phase (Peipei et al. 2004; Heughebaert et al. 1977; Blumenthal et al. 1972). Intense absorption bands of PO_4^{3-} groups have been found at 1045 cm^{-1} (ν_3 asymmetric stretching mode), 604 and 571 cm^{-1} (ν_4 bending mode). The ν_1 asymmetric

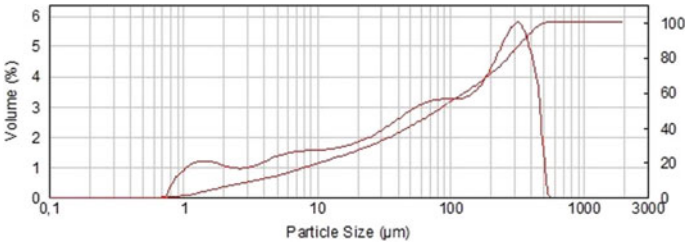

Fig. 4 Particle size distribution of as-dried powder P2 at 100 °C end 24 h

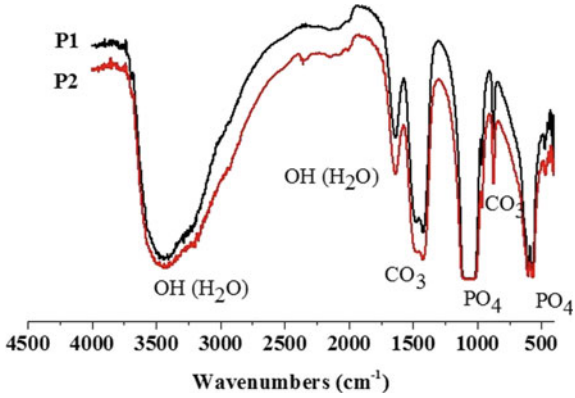

Fig. 5 FTIR spectra of as-dried powder P1 and P2 at 100 °C during 24 h

stretching mode at 960 cm^{-1} and ν_2 at 470 cm^{-1} is not observed in the sample P1. The absorption band at 1422 cm^{-1} is attributed to CO_3^{2-} groups (ν_3 stretching mode) which resulted from partial substitution of PO_4^{3-} groups by carbonate ions (B-type substitution). The presence of CO_3^{2-} groups in the lattice of apatitic phase formed is resulted from atmospheric CO_2 contamination during the precipitation process. The reactor exposed to air, medium alkaline reaction (pH > 8), and low precipitation temperature, which increases the solubility of CO_2 are the main factors that caused this contamination.

The reaction of atmospheric CO_2 dissolution in an alkaline medium is:

$$CO_2(g) + 2OH^-(aq) \rightarrow CO_3^{2-}(aq) + H_2O \quad (1)$$

The weak band at 874 cm^{-1} is attributed to CO_3^{2-} (A-type substitution) or HPO_4^{2-} groups (Moghimian et al. 2012). The high intensity bands at 3441 and 1641 cm^{-1} are attributed to absorbed water molecules. The absence of the bands at 3750 and 630 cm^{-1} characteristic of OH^- groups of hydroxyapatite is assigned to the substitution of these groups by carbonate ions. Although, Gema et al. (2018) have found the same result and indicate that the presence of strong carbonate bands in the range of 1400–1460 cm^{-1} and the band at 875 cm^{-1} implies the presence of AB type carbonated substituted apatites (Ca_{10-x} $(PO_4)_{6-x}$ $(CO_3)_x$ $(OH)_{2-x-2y}$ $(CO_3)y$).

The FTIR spectrum of the as-dried powder P2 is similar to that of powder P1. However, two supplementary bands have been identified at 960 cm^{-1} and 470 cm^{-1}, which are, respectively, attributed to $\nu_1$symmetric stretching mode and ν_2 bending mode of PO_4^{3-}. The broad band at 1045 cm^{-1} corresponding to PO_4^{3-} groups indicates that the synthetized apatite is poorly crystalline, which confirms the XRD results.

Infrared spectra of the powder P1 calcined at 600, 800, 1000, and 1100 °C are reported in Fig. 6. The absorption bands of OH groups of hydroxyapatite appeared at about 600 °C and all other peaks in the spectra were characteristics of hydroxyapatite.

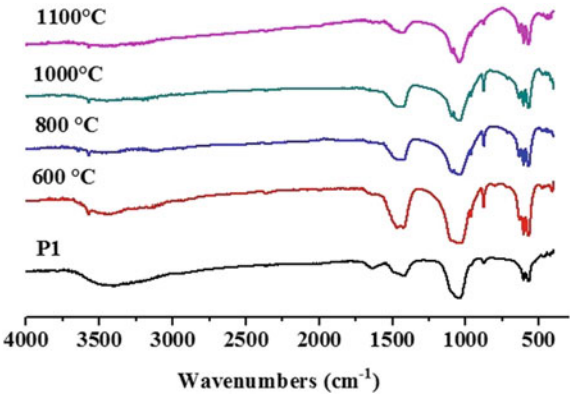

Fig.6 FTIR spectra of the powder P1: as-dried and calcined at 600, 800, 1000, 1100 °C for 1 h at 5 °C/min

The sharp peaks of PO_4^{3-} groups, when the calcination temperature increases, indicate that the crystallinity of hydroxyapatite increases. No decomposition of hydroxyapatite was observed even at 1100 °C, which confirms their stability (presence of OH groups at 3570 cm^{-1}) (Kang et al. 2019).The same result was obtained with the calcined powder P2 (Fig. 7).The diminution of the band at 1450 cm^{-1} is assigned to the decomposition of carbonate ions to form CO_2 (g).

The XRD spectra of the calcined powder P1 at 600, 800, 1000, and 1100 °C are reported in Fig. 8. In comparison with the as-dried powder, the crystallinity of the powders calcined at 800, 1000, and 1100 °C was raised and all the diffractions peaks correspond to the hydroxyapatite phase (ICDD N°96-900-2217). Low-intensity peaks at 37.44° and 54.55° in the DRX paterns of powder P1 calcined at 800, 1000 and 1100 °C are attibuted to CaO phase, which corresponds to the remained Ca $(OH)_2$ of the reaction or to the no total decomposition of carbonate ions present in the lattice of hydroxyapatite powder (Landi et al. 2004).

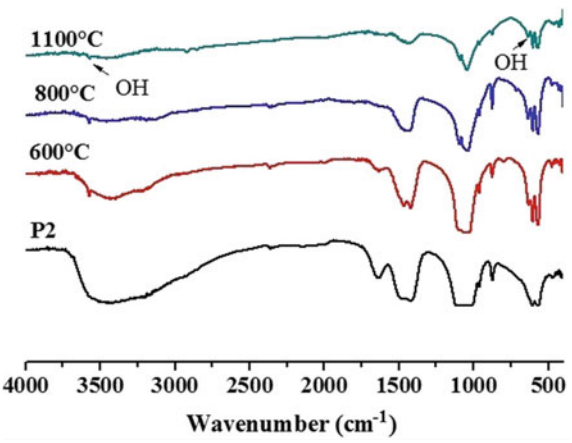

Fig. 7 FTIR spectra of the powder P2: as-dried and calcined at 600, 800, 1100 °C for 1 h at 5 °C/min

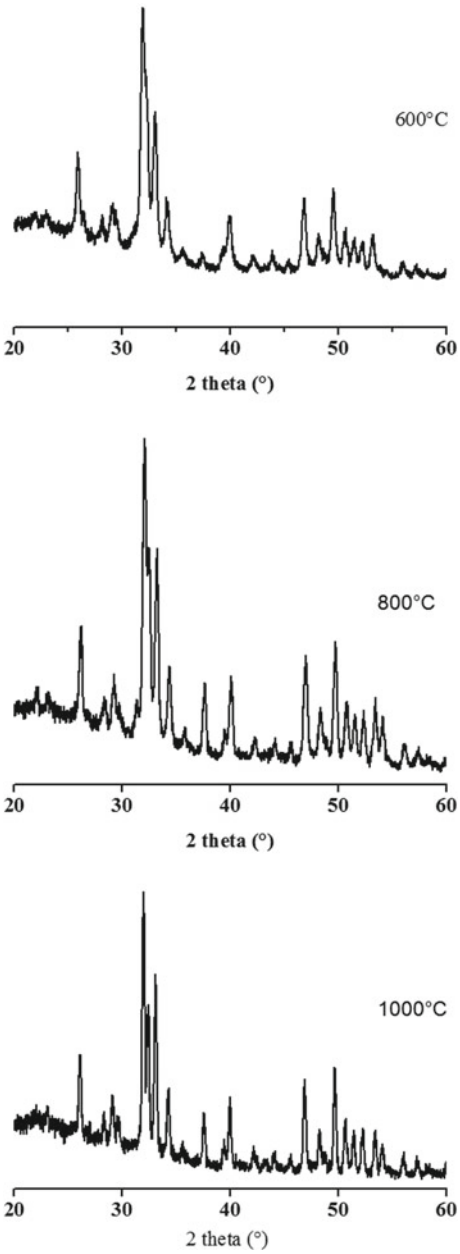

Fig. 8 DRX patterns of powder P1: as-dried and calcined at 600, 800, 1000, 1100 °C for 1 h at 5 °C/min

Fig. 8 (continued)

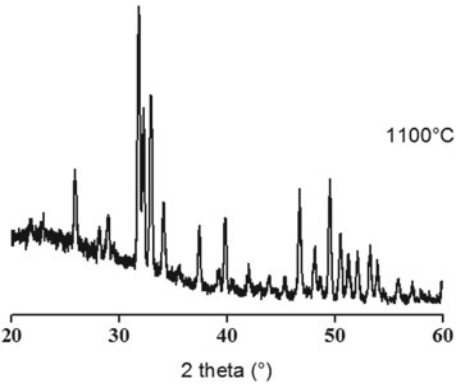

4 Conclusion and Future Perspective

Acid–base neutralization is an easy method to prepare hydroxyapatite powder by using $Ca(OH)_2$ and H_3PO_4 as precursors. The results of this work have shown that using rich calcium solution allows preparing hydroxyapatite at room temperature (23 °C) at reduced aging time (1 h) by the calcination of the obtained precipitate at 600 °C for 1 h. The particle size of the obtained powder depends on the concentration of the acidic solution. The evolution of pH of synthesis with time depends on the concentration of the acid solution as well. The obtained hydroxyapatite powder is stable even at high temperature of treatment. Depending on the application field of the synthesized powder, other properties are required to study in the future as the morphology of the particles, surface area, and porosity of the powder.

References

Azade Y, Suat Y (2018) Wet chemical precipitation synthesis of hydroxyapatite (HA) powders. Ceram Int 44:9703–9710

Blumenthal C, Posner AS, Holms JM (1972) Effect of preparation conditions on the propperties and transformation of amorphous calcium phosphate. Mat Res Bull 7:1181–1190

Doan PM, Haroun S, Ange N, Patrick S (2012a) Apatitic calcium phosphate: Synthesis, characterization and reactivity in the removal of lead (II) from aqueos solution. Chem Eng J 180–190

Doan PM, Nathalie L, Haroun S, Ange N, Sharrock P (2012b) Synthesis of calcium hydroxyapatite from calcium carbonate and different orthophosphate sources: a comparative study. Mater Sci Eng B 177:1080–1089

Doan PM, Sébastien R, Patrick S, Haroun S, Nathalie L, Ngoc DT, Mohamed R, Ange N (2014) Hydroxyapatite starting from calcium carbonate and orthophosphoric acid: synthesis, characterization, and applications. J Mater Sci 49(12):4261–4269

Elena L, Anna T, Giancarlo C, Lucia V, Monica S (2004) Influence of synthesis andsintering parameters on the characteristics of carbonate apatite. Biomaterials 25:1763–1770

Elhammari L, Merroun H, Coradin T, Cassaignon S, Laghzizil A, Saoiabi A (2007) Mesoporous hydroxyapatites prepared in ethanol–water media: structure and surface properties. Mater Chem Phys 104:448–453

Florin M, Aura-Catalina M, Catalina AD, Andreea M, Dan B, Andrei B, Stefan IV, Marian M, Vijay KT, Lucian TC (2017) Facile synthesis and characterization of hydroxyapatite particles for high value nanocomposites and biomaterials. Vacuum 146:614–622

Gema G, Cesar CV, Luis JB, Damarys S, Lisbeth L, Jose IC, Camilo JD, Luis L (2018) Effect of carbonates on hydroxyapatite self-activated photoluminescence response. J Lumin 195:385–395

Haifeng G, Changhua J, Zhenxuan X, Pingying L, Zhaofu F, Jia Z (2019) Synthesis of bitter gourd-shaped nanoscaled hydroxyapatite and its adsorption property for heavy metal ions. Mater Lett 241:176–179

Heughebaert J-C, Montel G (1977) Etude de l'évolution de l'orthophosphate tricalcique non cristalin en phosphate apatitique à la faveur d'une réaction chimique, à température ordinaire. Revue de physique appliquée. Tome 12

Kang S, Seo JT, Park S-H, Jung Y, Lee CY, Park J-W (2019) Qualitative analysis on crystal growth of synthetic hydroxyapatite influenced by fluoride concentration. Arch Oral Biol 104:52–59

Landi E, Tampieri A, Celotti G, Vichi L, Sandri M (2004) Influence of synthesis and sintering parameters on the characteristics of carbonate apatite. Biomaterials 25:1763–1770

Maya I, Madona L, Jean-M G, Jean-François L (2020) Hydroxyapatite, a multifunctional material for air, water and soil pollution control: a review materials. J Hazard 383:121–139

Mehdi SS, Mohammad-TK, Ehsan DK, Ahmad (2013) J Synthesis methods for nanosized hydroxyapatite with diverse structures. Acta Biomaterialia 9:7591–7621

Michele F, Sebastiano C, Marco S, Claudio E, Paolo C, Antonella G (2019) In-depth study of the mechanism of heavy metal trapping on the surface of hydroxyapatite. Appl Surf Sci 475:397–409

Moghimian P, Najafi A, Afshar S, Javadpour CJ (2012) Effect of low temperature on formation mechanism of calcium phosphate nano powder via precipitation method. Adv Powder Technol 23:744–751

Peipei W, Caihong L, Haiyan G, Xuerong J, Hongqiang W, Kaixing L (2010) Effects of synthesis conditions on the morphology of hydroxyapatite nanoparticles produced by wet chemical process. Powder Technol 203(2):315–321

Sangeetha K, Vidhya G, Vasugi G, Girija EK (2018) Lead and cademium removal from single and binary metal ion solution by novel hydroxyapatite/alginate/gelatin nanocomposites. J Environ Chem Eng 6(1):1118–1126

Souzaa FS, Matosb MJS, Galvãoa BRL, Arapiracaa AFC, Silvaa SN, Pinheiroa IP (2019) Adsorption of CO_2 on biphasic and amorphous calcium phosphates: an experimental and theoretical analysis. Chem Phys Lett714:143–148